Available online at www.sciencedirect.com
SCIENCE DIRECT®
ELSEVIER
Nuclear Instruments and Methods in Physics Research A 516 (2004) 34–49
NUCLEAR INSTRUMENTS & METHODS IN PHYSICS RESEARCH Section A
www.elsevier.com/locate/nima

Development of a scintillating-fibre detector with position-sensitive photomultipliers for high-rate experiments

S. Horikawa[a,d,*], I. Daito[b], A. Gorin[c], T. Hasegawa[d], N. Horikawa[b], T. Iwata[a,1], K. Kuroda[e], I. Manuilov[c], T. Matsuda[d], Y. Miyachi[a,2], A. Riazantsev[c], A. Sidorov[c], N. Takabayashi[a], T. Toeda[a]

[a] *Department of Physics, School of Science, Nagoya University, Furo-cho, Chikusa-ku, Nagoya 464-8602, Japan*
[b] *Center for Integrated Research in Science and Engineering, Nagoya University, Nagoya 464-8603, Japan*
[c] *IHEP, Protvino 142284, Russia*
[d] *Faculty of Engineering, Miyazaki University, Miyazaki 889-2192, Japan*
[e] *JINR, Dubna 141980, Russia*

Received 25 November 2002; received in revised form 19 June 2003; accepted 28 July 2003

Abstract

An extensive study was performed on the development of fast and precise scintillating-fibre detectors with position-sensitive photomultipliers (PSPM) for application in high-rate experiments. Several detector prototypes with Kuraray multi-cladding fibres of 0.5 mm diameter and Hamamatsu 16-channel H6568 PSPMs were constructed and tested under different beam conditions at the CERN PS and SPS beam lines. High time resolution of the order of 300 ps (r.m.s.) was obtained with spatial resolution of about 125 μm (r.m.s.) and with detection efficiency in excess of 98%. The detector prototype equipped with a 3-m-long light guide was also tested and showed a time resolution of about 540 ps (r.m.s.). Results of tests using a high-intensity muon beam show excellent stability of the detector performances in time and spatial resolutions as well as in detection efficiency under beam fluxes of up to 1.4×10^8 muons per 2.4-second spill.

PACS: 29.40.Gx; 29.40.Mc; 85.60.Ha

Keywords: Scintillating fibre; Position-sensitive photomultiplier; High-rate detector; Time resolution

1. Introduction

Scintillating-fibre (SciFi) detectors, developed over the last 10 years, have come into use for the tracking of charged particles in recent experiments [1–7].[3] They have a wide range of specifications,

*Corresponding author.
E-mail address: Sosuke.Horikawa@cern.ch (S. Horikawa).
[1] Present address: Department of Physics, Yamagata University, Yamagata 990-8560, Japan.
[2] Present address: Department of Physics, Tokyo Institute of Technology, Tokyo 152-8551, Japan.

[3] Among many works on SciFi detectors, Refs. [1–7] provide a partial list of recent papers about particle tracking.

0168-9002/$ - see front matter
doi:10.1016/j.nima.2003.07.038

mainly in terms of the photosensitive devices employed. The RD17 (FAROS) Collaboration at CERN has demonstrated particularly high performances of SciFi detectors with position-sensitive photomultipliers (PSPM) [8]. Its work has consequently led to new applications of the SciFi technique in tracking detectors and also in *topological trigger* devices.

The idea to develop SciFi detectors with PSPMs in order to satisfy stringent conditions in recent high-rate experiments is essentially based on their two prominent features: good time resolution and high-rate capability due to the fast response of SciFis and PSPMs. Thanks to rapid progress achieved in recent years in the technology of both SciFis and PSPMs the performances of SciFi detectors have significantly improved, as demonstrated in the DIRAC (PS212) experiment at CERN [9].

In order to use this progress to benefit the COMPASS (NA58) experiment at CERN [10], research and development work has been done [11,12]. The final detectors have been in operation since 2000 and preliminary results are reported in Ref. [13]. The purpose of the present paper is to present some basic results which have demonstrated the feasibility of constructing such detectors to work under the severe conditions imposed by COMPASS.

One of the major physics goals of COMPASS is to determine the gluon polarization $\Delta G/G$ in the nucleon by measuring the cross-section asymmetry for open charm production in deep inelastic scattering of polarized muons on polarized nucleons. The low cross-sections for the interactions to be studied require high beam rates of the order of 2×10^8 muons/2.4-second spill. Covering the beam regions, SciFi trackers should be capable of measuring the incident and scattered muon tracks with a precision of a few hundred micrometres. In addition, accurate timing determination is particularly important for these trackers to select the triggered events amongst 10^8 incoming muons/s by means of the timing correlation. Time resolution better than 500 ps (r.m.s.) is thus required in order to keep the probability of accidental coincidences down to 10%.

In the present study, we investigate the overall performance of SciFi detector prototypes by the simultaneous measurements of various parameters: time and spatial resolutions, detection efficiency and hit multiplicity. One of the most important subjects in the present paper is the test of the prototype under high-rate conditions. The prototype using Hamamatsu H6568 PSPMs equipped with a booster was tested under high rates up to 4 MHz/fibre-channel, showing stable performances. In parallel, Bisplinghoff et al. [14] performed high-rate tests of a SciFi detector consisting of SciFis of 1 mm diameter. They showed that the output pulse height is stable up to rates of several 10^6 Hz/fibre-channel when the PSPM tube is equipped with a booster base. This is in agreement with the stability in detector performances we present here. Radiation hardness of the fibres, which is the other essential issue for the high-rate application of SciFi detectors, was also studied in detail in Ref. [14].

In Section 2, we describe the detector design and the readout electronics. In Section 3, we present test results of basic performances obtained from the detector prototypes with different configurations. Section 4 is devoted to test results under high-rate conditions with a beam flux of up to 1.4×10^8 muons/spill. Some discussion and conclusions are given in Section 5.

2. Description of the detector

2.1. Structure of the fibre bundle

Two different fibre bundles, H7 and H13, were prepared especially to study the dependence of the time resolution on the number of photons generated in the fibres. They differ in the number of SciFis aligned along the direction of incident particles, and in the length of clear fibres connected as light guides between SciFis and a PSPM.

The structure of a SciFi array is shown in Fig. 1. Both H7 and H13 consist of two precisely overlapped planes, A and B, each containing 16 fibre columns of Kuraray SCSF-78MJ multi-cladding SciFis of 0.5 mm in diameter [15]. We previously demonstrated that the use of multi-cladding fibres ensures higher light yield and is a good solution to

improve the time resolution [12]. The number of layers per plane is 7 and 13 for H7 and H13, respectively. Each pixel of the detectors is therefore defined by 7 or 13 fibres precisely aligned along the incident particle direction. The fibre columns are most closely packed in the direction perpendicular to the beam, resulting in a pitch of 0.43 mm between adjacent fibre columns. The scintillating cores (0.44 mm in diameter) of SciFis in adjacent columns are thus slightly overlapped so that the fibre array is continuously sensitive to incident particles without dead space.

Fig. 2 shows the basic concept of a single-detector plane. Each individual SciFi is connected with optical epoxy to a clear fibre (Kuraray Clear-PSM) of the same diameter. Connection of scintillating and clear fibres is made with the aid of a jig consisting of a brass plate with grooves of pitch 0.86 mm precisely machined on its surface. The two fibres, rectified at the ends, are introduced into grooves from opposite sides, and glued with optical epoxy. During hardening of the epoxy, fibres are kept tightly inside the grooves by other parts of jig so that the fibre ends are precisely placed face-to-face over all the pairs of fibres to be glued. Using this technique we were able to glue precisely more than 50 pairs of fibres with a single cycle of the procedure, resulting in a large time saving compared to the welding of fibre pairs one by one. The same technique was recently employed with success in the construction of high-resolution hodoscopes using fibres of 0.28 mm diameter [16].

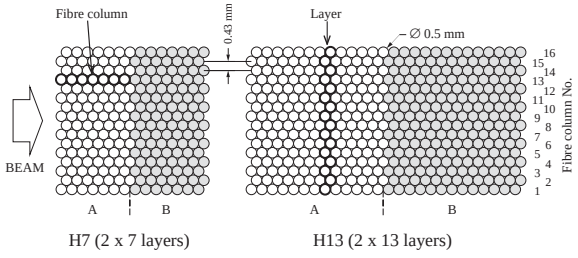

Fig. 1. Structure of a SciFi array.

The far ends of clear fibres are grouped for each fibre column and glued inside a hole perforated in a black plastic diskette designed to keep the fibre ends precisely positioned at the centre of each pixel of the PSPM and in good contact with the photocathode window. The light pulses yielded in a fibre column are thus led to the corresponding PSPM pixel, and then read out by an individual

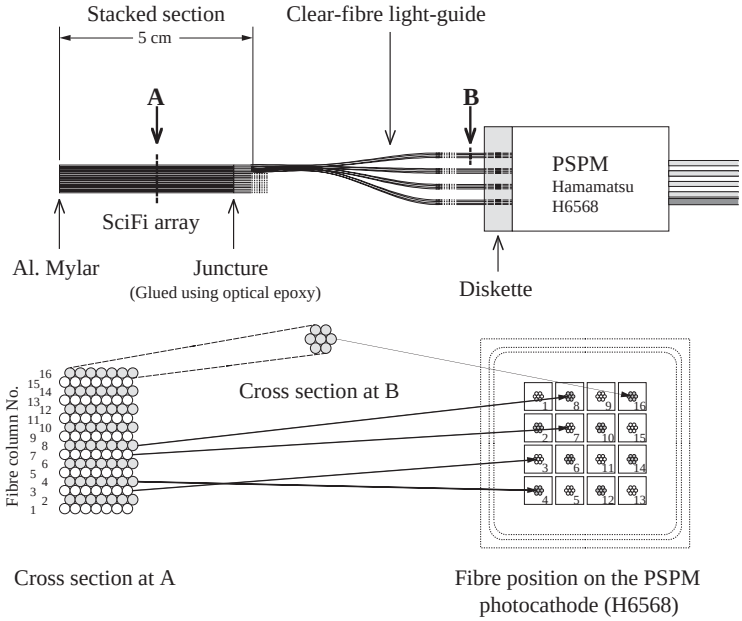

Fig. 2. Concept of a single detector plane.

channel of associated electronics. A sheet of aluminized Mylar is glued using optical epoxy on the open side edge of the fibre array and serves as a reflector.

Some of the SciFi trackers in the COMPASS spectrometer are located close to the superconducting solenoid magnet of the polarized target. Light guides with a length of a few metres are therefore needed for these trackers to keep the PSPM away from the magnets to prevent the deterioration of the PSPM output signal due to the strong fringe field. The feasibility of using long light guides for this purpose was demonstrated in Ref. [11]. For the present study, we prepared additional light guides of 3 m length to be inserted between the H7 fibre bundle and the PSPM so that we can investigate directly the effect of the long light guides. Such a light-guide extender is made of 16 Kuraray Clear-PSM fibres 2.0 mm in diameter for each plane of H7. As illustrated in Fig. 3, seven clear fibres, corresponding to each SciFi column, are connected to an individual clear fibre of the extender with the aid of precisely perforated holes on the diskettes. For reasons of mechanical stability, connection of the fibre components as mentioned above is made without any optical medium, such as optical grease, following experimental confirmation that the loss of light across the air gap at the joints is only of the order of 10%. This is a far simpler solution than the connection of 0.5 mm fibres as described in the preceding paragraph when there is no strict constraint on the lateral position of fibres to be connected.

Table 1 summarizes the different detector prototypes investigated in the present study.

2.2. Position-sensitive photomultiplier

The choice of the photomultiplier tube was made taking into account the excellent characteristics of

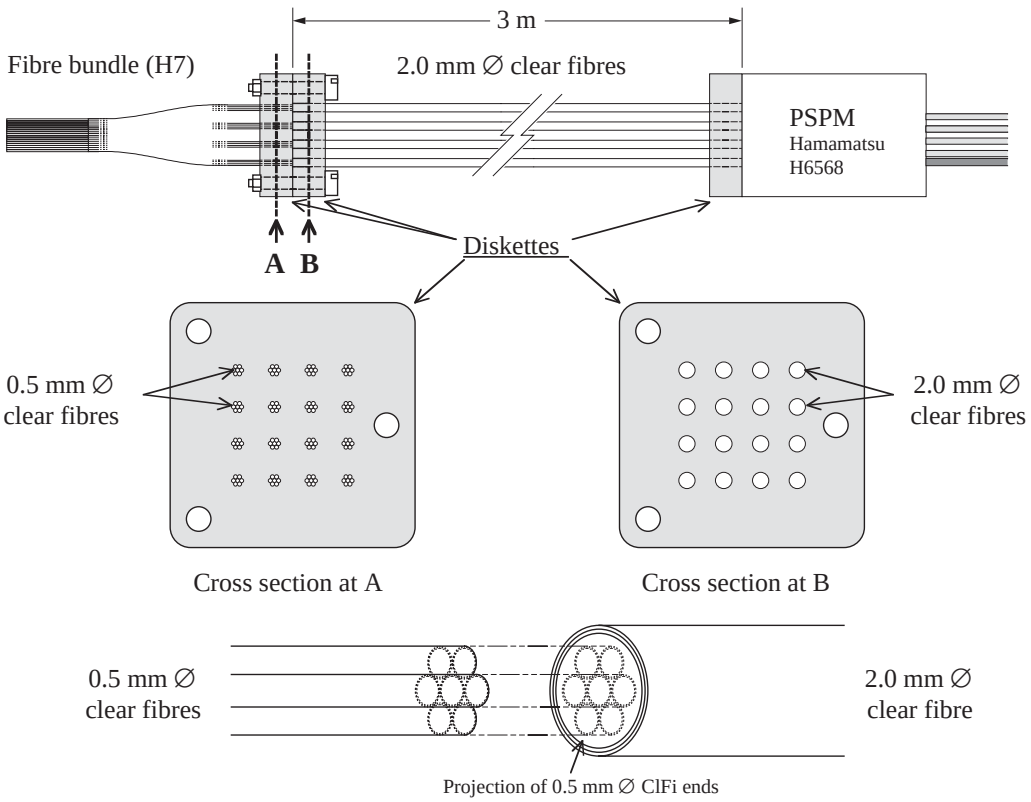

Fig. 3. Concept of the light-guide extender.

Table 1
Detector configurations

Detector	Fibre bundle				LG extender
	Description	No. of layers per plane	SciFi length (0.5 mm ϕ)	ClFi length (0.5 mm ϕ)	ClFi length (2.0 mm ϕ)
H7	H7	7	5 cm	50 cm	—
H7L	H7	7	5 cm	50 cm	300 cm
H13	H13	13	5 cm	25 cm	—

Abbreviations: ClFi—Clear Fibre; and LG—Light Guide.

the H6568 from Hamamatsu Photonics [17] already confirmed in the DIRAC experiment. H6568 is a type number of a photomultiplier tube assembly including the housing, integrated voltage divider and signal cables provided by the manufacturer. The bare tube is called R5900-00-M16, which is known for its high performances in single photon detection with practically no noise and has been used for various experiments in, for example, RICH counters [18]. It also has good time characteristics, such as a typical anode pulse rise time of 0.83 ns with a transit time spread of 0.3 ns (FWHM). The typical gain of the tube is about 3×10^6 at a high voltage of HV = 800 V and about 10^6 at HV = 700 V, which allow us to use them without amplifiers. In addition, this tube shows a high immunity to the external magnetic field as described in Appendix A.

Our PSPMs differ from the tube commercially available in this series by the following specifications. They are equipped with an output of the last dynode signal, and four booster cables from the last four dynodes. The last dynode output provides the analog sum of all 16 anode signals, which can be used as a monitor of signal amplitudes as well as for trigger purposes. The four booster cables allow us to provide independent booster voltages, stage by stage, in order to minimize the gain drop due to the increase of the dynode current under very high-rate conditions.

2.3. Peak-sensing circuit discriminator

A peak-sensing circuit (PSC) is a type of discriminator sensitive to the variation of pulse amplitude across adjacent channels [19]. It is designed for the readout of anode signals of PSPMs, particularly in combination with SciFi detectors. The initial motivation for PSC development was to treat in real time a strong cross-talk between adjacent channels of first-generation PSPMs. However, recent progress in the PSPM technology has reduced the internal cross-talk due to the dispersion of secondary electrons to a few per cent. The main source of cross-talk in the present case is, therefore, the tracks traversing the slightly overlapping adjacent fibre columns and/or transmission of photons between them (see Section 3.2). With properly tuned thresholds, a PSC allows the annoying effects of the cross-talk between adjacent channels to be suppressed and the track position to be defined in real time as demonstrated in Ref. [19]. In comparison with a conventional threshold discriminator, a PSC gives fewer multi-hits while better maintaining the detection efficiency. Such an electronics is particularly useful to define a *topological trigger* in high-rate experiments without the hindrance of a high multiplicity of hits due to the cross-talk. In the present application, a low multiplicity of hits per event significantly helps to simplify the position information of incident particles.

For the first part of the present study, we used a PSC module designed for the DIRAC experiment. For the tests under high-flux beam, described in Section 4, PSC prototypes recently developed for the COMPASS experiment were used. The new module, realized in the 3U euro-mechanics standard, houses 16 inputs and 16 digital outputs. The output pulse is in the LVDS level and the width is $\sim$8 ns. Dead time is reduced to $\sim$7 ns for application in high-rate experiments, resulting in a double pulse resolution of the order of 15 ns. The discriminator threshold in each channel can be

adjusted within a range from 5 to 100 mV via PC remote control based on the RS485 protocol, capable of handling 8×31 discriminator units. The tuned threshold values can be memorized in an 8-bit EEPROM chip. In addition, an inverting amplifier with a gain of the order of 10 is integrated in the same module for an analog output of the last dynode signal. The specifications of the PSC discriminator are summarized in Table 2.

Table 2
Specifications of a PSC discriminator for the COMPASS SciFi trackers

Parameter	Value/description
Input	16 channels, negative
Input impedance	50 Ω
Output	16 twisted pairs
Output impedance	100 Ω
Output pulse level	LVDS
Output pulse width	8 ns
Double pulse resolution	~15 ns
Threshold level range	5–100 mV
Remote protocol	RS485
Height	3U

3. Basic performances of different detector prototypes

3.1. Experimental conditions

We carried out a test experiment on the T11 beam line of the Proton Synchrotron (PS) at CERN. Three detector prototypes described in Section 2, namely H7, H7L and H13, were exposed to 3.6 GeV/c positive hadrons with a maximum intensity of about 10^6 particles/spill (1.5 s).

Fig. 4 presents the detector layout of the test experiment. The three detector prototypes were successively investigated under similar conditions. The two overlapped planes of each detector were used for simple and precise tracking, i.e. the tracking plane (B or A) is used to define the track position needed to investigate the performances of the other plane (A or B). B1 and B2 are trigger counters using relatively large plastic scintillator

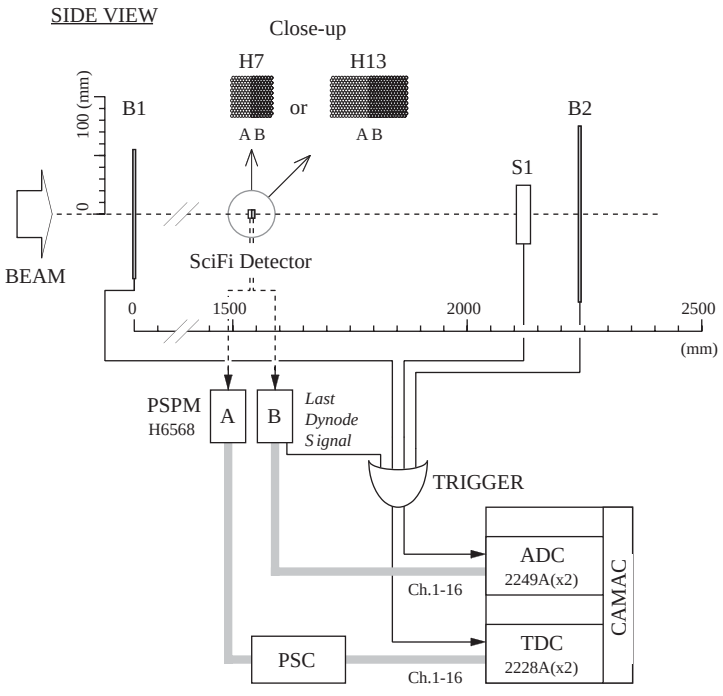

Fig. 4. Experimental set-up on the T11 beam line.

plates with an area of about 11×11 and $15 \times 15\ cm^2$, respectively. S1 is also a trigger counter, having a width of 15 mm in the direction parallel to the fibres. The last dynode signal from the tracking plane was also included for the trigger. The typical trigger rate was about 10^3 events/spill at a beam flux of about 10^5 particles/spill.

For most of the measurements, we adopted the following readout scheme. PSPM anode signals from one of the overlapping planes (B or A) were directly sent to CAMAC Analog-to-Digital Converters (ADC), LeCroy 2249A, via 30-m-long coaxial cables. At the same time, the other plane (A or B) was connected to CAMAC Time-to-Digital Converters (TDC), LeCroy 2228A, through a PSC discriminator. Time binning of the TDC was set to 50 ps. PSC output signals were sent to the TDC via a 10-m-long twisted-pair flat cable. For some dedicated measurements, like time resolution, each plane was connected to a PSC followed by two TDCs.

3.2. Amplitude spectra

Amplitude spectra were measured to determine the number of photoelectrons produced in each detector. Fig. 5 shows an example of raw amplitude spectra obtained with an ADC for fibre channel No. 8 of plane A of H7, H7L and H13. The pedestal-peak position corresponds to 0 in ADC amplitude.

The raw amplitude spectra are characterized by a unique shape containing two prominent peaks. The first one is around the 10th ADC channel and corresponds to the single photoelectron peak produced mainly by events in which a significant light signal is yielded in one of the adjacent fibre columns. Such a small light cross-talk might easily be caused by inclined tracks traversing partially (or grazing) the column in question and/or by transmission of photons from the adjacent columns. The second wide peak is produced by the particles traversing the full column. To obtain the spectra shown in Fig. 6, we selected good events in which only the corresponding column of plane B was fired. The single photoelectron peak is totally suppressed and the distribution forms a broad Gaussian-like peak as expected. We find these peaks are very well separated from the single photoelectron peak. The number of photoelectrons for each fibre detector can be roughly estimated by the ratio of mean values of the two

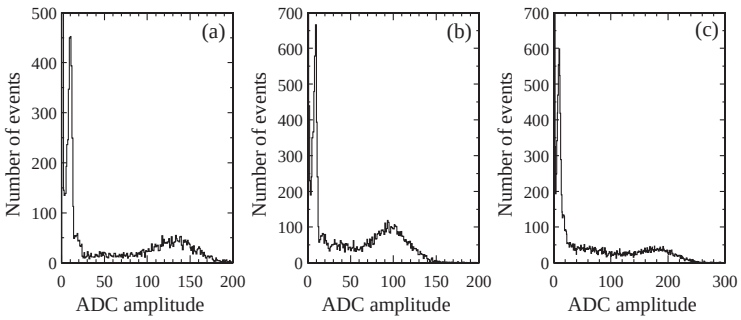

Fig. 5. Raw amplitude spectra obtained from (a) H7, (b) H7L and (c) H13.

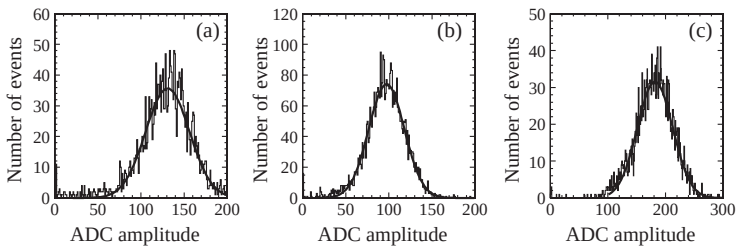

Fig. 6. Amplitude spectra obtained from (a) H7, (b) H7L and (c) H13, after an event selection.

peaks assuming the linearity of the PSPM. We thus obtained ~14, ~10 and ~22 photoelectrons for H7, H7L and H13, respectively, as an average over all the active channels. It should be noted that we can directly estimate the effect of the light-guide extender by comparing the results obtained from H7 with and without the extender. The attenuation in the 3-m-long clear fibres is thus roughly estimated to be 30%.

3.3. Local detection efficiency and hit multiplicity

The local detection efficiency and the hit multiplicity per event were studied for each plane (A or B) connected to a PSC with the aid of the tracking plane (B or A) connected to ADCs. The hit-fibre column on the tracking plane was defined by the channel giving the maximum amplitude among all the active channels.

Two types of local detection efficiency were then defined as follows. The first, one-to-one efficiency, is the probability to find a hit in the column of the investigated plane corresponding to the hit-fibre column defined in the tracking plane. The second type, one-to-three efficiency, is the probability of at least one hit among three columns centred on the corresponding one.

Fig. 7 shows an example of the results obtained for each plane A and B of H7. It should be noted that both efficiencies are slightly low at the extremity channels due to a geometric effect at the detector edges. The average value over the remaining 14 channels of the one-to-one efficiency is about 95%, and that of the one-to-three efficiency is as high as 98%. Taking into account the angular divergence and multiple scattering of incident particles, we consider that the one-to-three efficiency is a reasonable measure of the local efficiency.

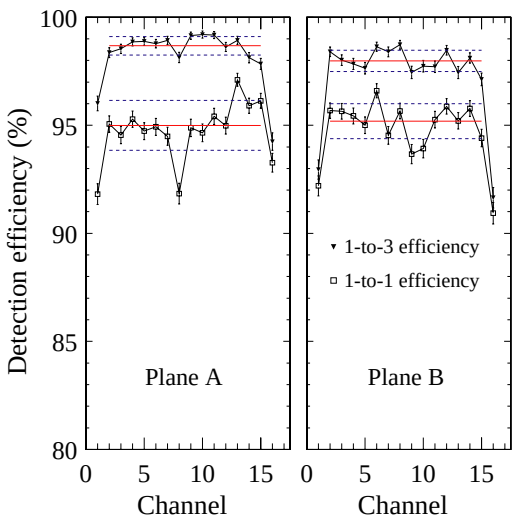

Fig. 7. Local detection efficiency of planes A and B of H7.

The hit multiplicity is defined simply by the number of hits observed on the investigated plane (A or B) for a single track detected by the tracking plane (B or A). This quantity is related to the cross-talk between columns and also the noise of the PSPM, and therefore strongly depends on adjustment of the PSC thresholds. In order to perform a good tracking, it is important to make a compromise between this quantity and the detection efficiency by optimizing the high voltage and/or discriminator thresholds. For a direct comparison of different detector prototypes in time and spatial resolutions all the detectors were tuned so as to have similar performances in detection efficiency and hit multiplicity.

The hit-multiplicity distributions on plane A of the three detectors H7, H7L and H13 obtained after such tuning are shown in Fig. 8. The global detection efficiency indicated in each plot is calculated from the ratio of the zero-hit events. The optimum high voltage on each detector was set so as to obtain a one-to-three efficiency higher than 97.5% with a multiplicity less than 1.2.

It can be estimated by a simple calculation that the detection efficiency does not depend much on the incident track angle: up to ± 300 mrad, for example, in the case of H7. In addition, the adjacent double-hit events, where the inclined track traverses simultaneously two adjacent fibre columns, can be suppressed by using a PSC. Taking into account the results reported in Ref. [20][4] on the measurement of angular dependence

[4] The angular dependence of the multiplicity and of the detection efficiency have been studied with an array of square fibres of 2×2 mm^2, each connected to a PSPM channel [20]. Neither quantity depends very much on the incident angle up to 45° (corresponding to the diagonal of the fibre section), but beyond this angle the number of multiplicity-2 events increases rapidly due to two adjacent elements simultaneously crossed by a single incident particle.

of the multiplicity as well as the detection efficiency, we estimate that the multiplicity does not change much up to an incident track angle of about ± 100 and ± 50 mrad for H7 and H13, respectively. It should also be noted that, in the COMPASS case, the maximum angular acceptance required for SciFi trackers is ± 25 mrad.

3.4. Time resolution

The time resolution was measured by using a PSC followed by TDCs for each of planes A and B. The high voltage for each PSPM was set so as to optimize the tracking performances as described in Section 3.3. Fig. 9 shows the distributions of events as a function of the time difference between the TDC contents of the corresponding fibre channels, No. 8 of planes A and B. Assuming that the time resolution is similar for the two planes, that of a single plane is calculated from the widths of the distributions as shown in Fig. 9 divided by $\sqrt{2}$. The time resolution obtained in such a way is plotted in Fig. 10 for different fibre channels. The average values over all the active channels are ~ 300 (r.m.s.), ~ 540 (r.m.s.) and ~ 280 ps (r.m.s.) for H7, H7L and H13, respectively. The time resolution is clearly impaired in H7L by attenuation and dispersion of the light signals in the 3-m-long light guide. It should be noted that the time resolution was measured also by irradiating the full length of the fibre array by excluding S1 from the trigger, and the results showed practically no deterioration due to the

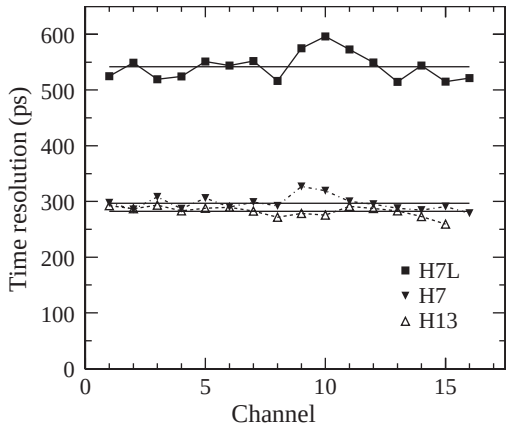

Fig. 10. Time resolution of different fibre channels in each detector prototype.

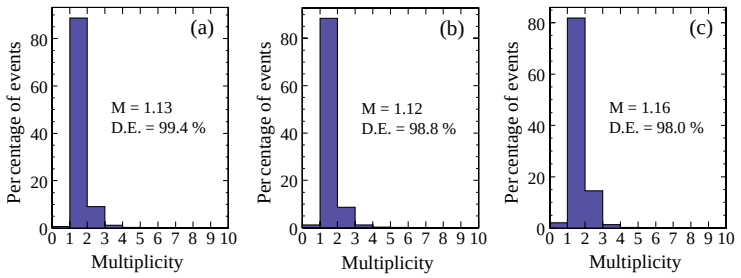

Fig. 8. Hit-multiplicity distribution on plane A obtained from (a) H7, (b) H7L and (c) H13 after tuning. Values of multiplicity (M) and detection efficiency (DE) are indicated.

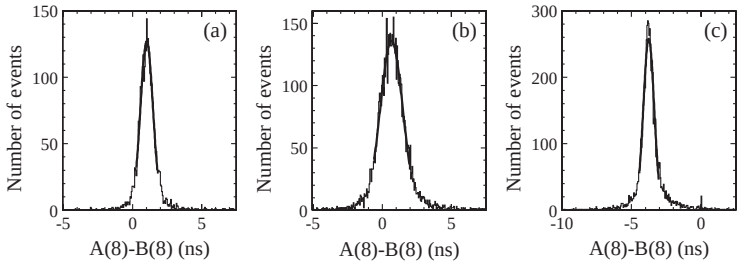

Fig. 9. Time difference distribution obtained from (a) H7, (b) H7L and (c) H13.

propagation of the light across the 5-cm-long fibres.

3.5. Spatial resolution

The spatial resolution was studied by connecting plane B to ADCs and plane A to TDCs through a PSC. Fig. 11 presents a correlation plot of the tracks detected in plane A against those defined in plane B of the H7 detector. Almost all the tracks in one of the plane B channels fall inside the corresponding plane A channel. The equivalent resolution is therefore given by $0.43\,\text{mm}/\sqrt{12} \approx 125\,\mu\text{m}$ (r.m.s.).

Fig. 12 presents the track distributions on plane A for the events detected by one of the channels of plane B obtained from the H7, H7L and H13 prototypes. The event distribution is wider in H13 than in H7 or H7L, probably due to the angular divergence and multiple scattering of incident particles inside the thicker scintillator medium.

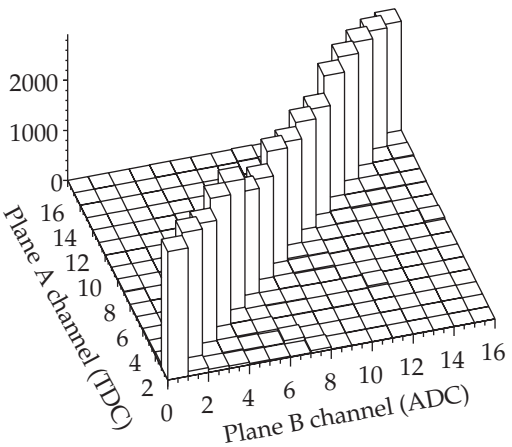

Fig. 11. Correlation plot of the tracks detected in plane A against those defined in plane B of the H7 detector.

3.6. Optimization of detector parameters

An exercise was performed using the H7 detector to find the optimum conditions of the PSC discriminators. Fig. 13 presents three essential parameters, namely time resolution, detection efficiency and multiplicity, plotted as a function of the high voltage applied on the PSPM. For a given high voltage, all the parameters were measured simultaneously with the aid of the overlapped planes A and B, each connected to TDCs through a PSC discriminator. The PSC

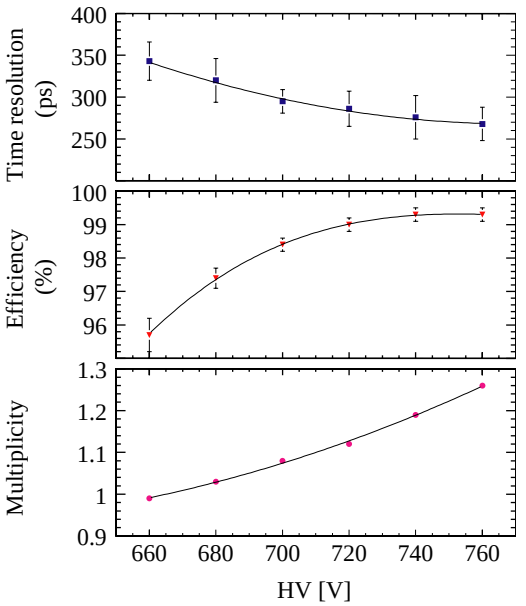

Fig. 13. High-voltage dependence of the detector parameters.

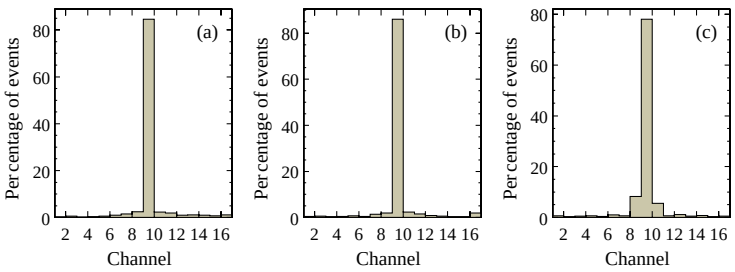

Fig. 12. Track distribution obtained from (a) H7, (b) H7L and (c) H13.

thresholds were kept constant during this measurement. It is clearly seen that higher voltage provides a better time resolution and a higher detection efficiency, but with increased multiplicity. Such an increase of the multiplicity would lower not only the spatial resolution but also the reconstruction efficiency of events detected under real experimental conditions. To avoid this problem the multiplicity should be kept to less than 1.1, as is obtained at a high voltage of about 700 V. The detection efficiency at this high voltage is still as high as 98.5%. It should be noted that the variations of the parameters shown in Fig. 13 reflect those obtained as a function of the PSC threshold at a fixed high voltage. In this interpretation, a higher value of the high voltage in Fig. 13 corresponds to a lower value of the threshold.

The same parameters were measured by compensating for the effects of increasing the high voltage with the aid of proper adjustment of the PSC thresholds. By maintaining the detection efficiency at 97.5% for example, it was possible to keep the time resolution and the multiplicity almost constant over a wide range of high voltages from 580 to 800 V. This means that SciFi detectors can be operated with fairly low high voltage on the PSPM, so as to ensure a better linearity of PSPM signals at lower space-charge effects. This is particularly important to perform high-intensity measurements with a good stability of the tracking performances.

4. Performances under high-rate conditions

4.1. Experimental conditions

In order to study the performances of SciFi detectors under extremely high-rate conditions we performed an additional test based on the M2 beam line of the CERN-SPS. In this study, the H7 detector was exposed to the 190 GeV/c muon beam with a flux of up to 1.4×10^8 muons/spill (2.4 s). The detector layout was similar to that shown in Fig. 4. The fibre array was placed on the focal point so that incident muons penetrate the two overlapped planes A and B with maximum rates.

For this study, special trigger counters were prepared by using separately A and B planes of the H13 prototype to replace B1 and B2 (see Fig. 4). Incident particles were defined by using only a single-fibre column of each A and B plane oriented in the direction perpendicular to the fibre alignment of H7 so as to have reasonably low trigger rates. The typical rate was about 2×10^5 events/spill.

For all the PSPMs used for H7 and H13, booster voltages were provided for the last four stages of the dynodes by connecting each dynode to an independent high-voltage power supply channel.

Most of the results presented in this section were obtained with the aid of the overlapped planes A and B, each connected to a PSC followed by a LeCroy 3377 multi-hit TDC.

In order to see how the high beam flux affects the detector performances some results were obtained twice: under low ($\sim 1 \times 10^7$ muons/spill) and high intensities ($\sim 1.4 \times 10^8$ muons/spill).

Fig. 14 shows a beam profile on the H7 for the high-intensity beam. The counting rate in each channel was estimated from the average number of hits inside a TDC time window opened by a random trigger. The maximum value of the order of 4 MHz was obtained in the central channels and the average over the full plane was about 3 MHz per channel.

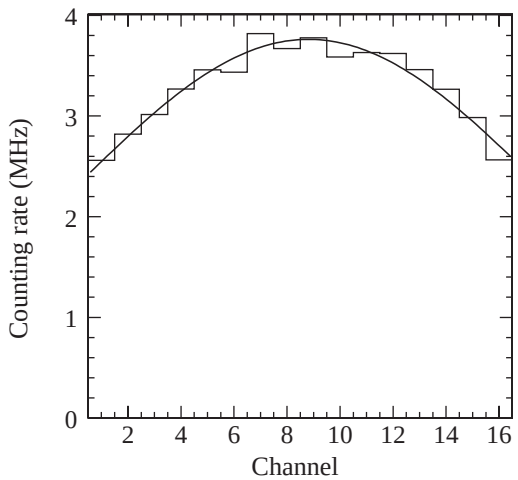

Fig. 14. Beam profile for the high-intensity beam with a flux of 1.4×10^8 muons/spill.

4.2. Amplitude spectra

Stability in pulse height of the signals from PSPMs is one of the essential performances of the present prototypes. Amplitude spectra were measured by connecting the anode output from plane A directly to ordinary CAMAC ADCs (2249A). Fig. 15 presents the spectra obtained from fibre channel No. 8 under high and low beam intensities. We selected the events by requiring only one hit detected in the corresponding channel of plane B within a time window as wide as the ADC gate duration of 25 ns. The counting rate of $\sim$4 MHz in this channel under the high beam intensity probably causes pile-up of the signals of the order of 6%. This results in a small bump on the higher tail of the spectrum shown in Fig. 15(a), which implies a contamination of the spectrum by such pile-up signals.

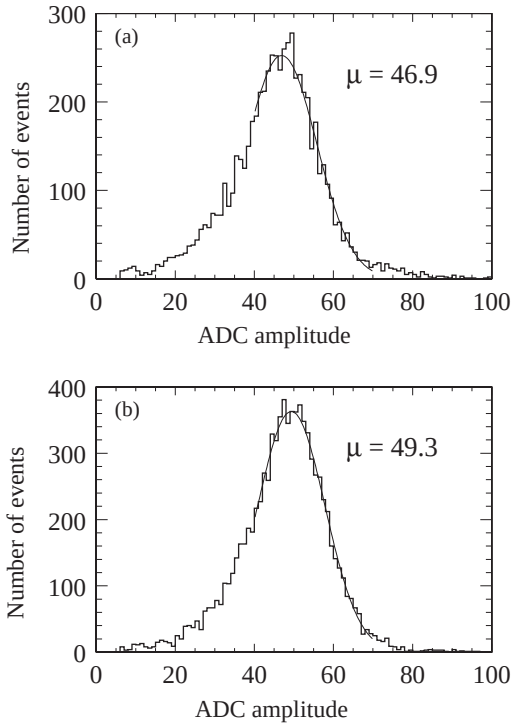

Fig. 15. Amplitude spectra obtained under (a) high (1.4×10^8 muons/spill) and (b) low (1×10^7 muons/spill) beam intensities after an event selection.

4.3. Local detection efficiency and hit multiplicity

As described in Section 3, the PSCs connected to planes A and B of H7 were tuned so as to settle a reasonable value in the multiplicity and the detection efficiency, before measuring other performances. The tuning was done by adjusting the PSC thresholds, channel by channel, for a given high voltage of the PSPMs, under the low beam intensity so that the probability of accidental hits in the time window of the TDC is negligible. The conditions imposed in this tuning are a multiplicity of less than 1.1, and a one-to-three efficiency of about 97.5% over the full range of the plane.

The detection efficiency was measured also at high intensity so as to confirm the stability under both beam conditions. The results obtained under the high beam flux of 1.4×10^8 muons/spill are shown in Fig. 16. The one-to-three efficiency is about 97%, except at the extremities where it is slightly lower as can be seen in Fig. 7.

Fig. 17 presents an example of the hit-multiplicity distributions obtained from plane A of H7 under high and low beam intensities. In order to study the level of hit multiplicity due to accidental tracks, we selected the events in which at least one

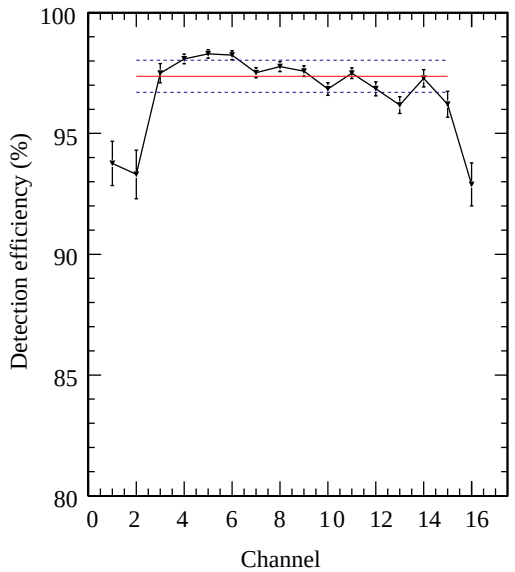

Fig. 16. Local detection efficiency (one-to-three efficiency) of the H7 plane A under high beam intensity.

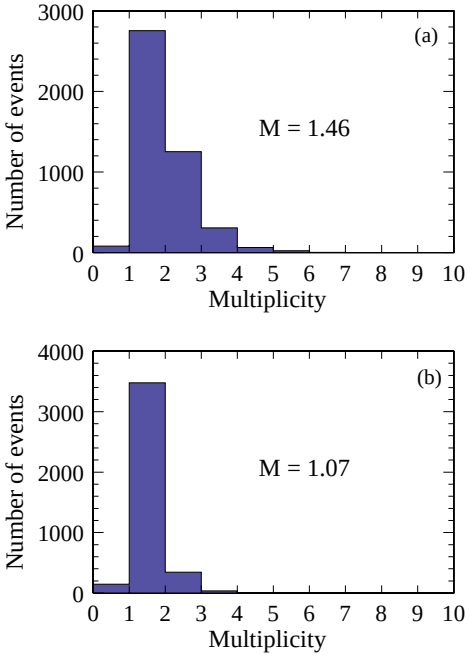

Fig. 17. Hit-multiplicity distribution obtained from H7 plane A under (a) high (1.4×10^8 muons/spill) and (b) low (1×10^7 muons/spill) beam intensities.

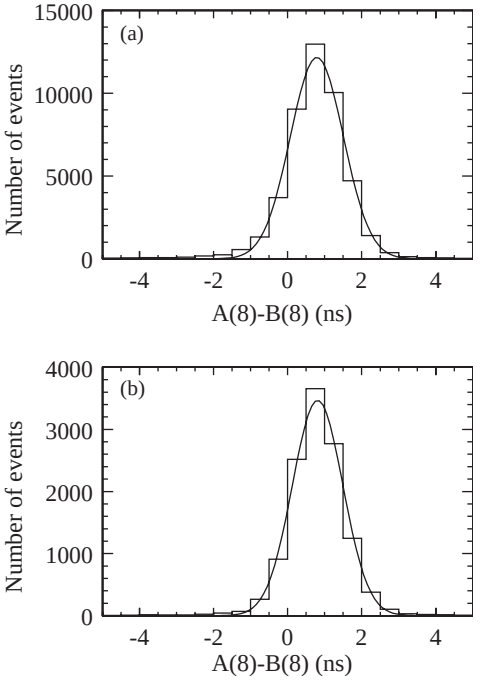

Fig. 18. Time difference between planes A and B of H7 obtained under (a) high (1.4×10^8 muons/spill) and (b) low (1×10^7 muons/spill) beam intensities.

hit was found in tracking plane B. The applied time window was of the order of 10 ns for both planes.

4.4. Time resolution

Typical examples of results on the time resolution obtained under high and low intensities are shown in Fig. 18. The number of events detected by the corresponding fibre channels, No. 8 of both the A and B planes, is plotted as a function of the time difference between the TDC contents of the two channels. Dividing the widths (r.m.s.) of such distributions by $\sqrt{2}$, we obtained $\sim$490 ps with high flux and $\sim$460 ps with low flux, as an average over 16 fibre channels. These numbers indicate that the time resolution is not significantly impaired at higher beam intensity. Taking into account the time resolution of the LeCroy 3377 TDC of the order of 300 ps, the intrinsic resolution of H7 is roughly estimated to be better than 400 ps. This estimate agrees with the time resolution of the order of 370 ps obtained under high intensity later using a dedicated multi-hit TDC for COMPASS data-taking (F1-TDC) [21], which has a better time resolution of $\sim$100 ps [13].

4.5. Spatial resolution

The spatial resolution was also studied under high-rate conditions by selecting the events each giving only a single hit on plane B. A time window of the order of 10 ns was applied for both planes to select the correlated events. Fig. 19 shows a correlation plot of the track positions thus detected by planes A and B of H7 under the beam intensity of 1.4×10^8 muons/spill. The background level is very low and a clear one-to-one correlation of the track positions is seen even under such high-intensity conditions. The spatial resolution is of the order of 125 μm as it was measured at low beam intensity, showing an excellent stability in its tracking performances.

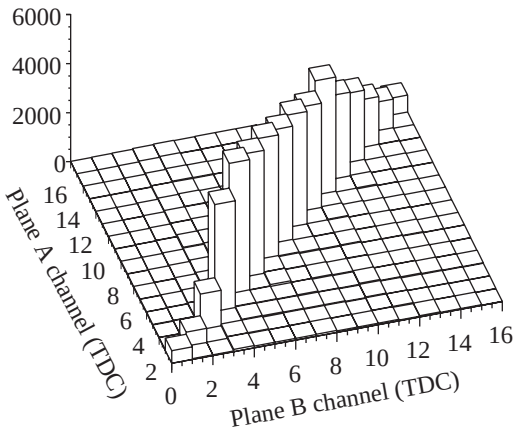

Fig. 19. Correlation plot of the track positions detected by planes A and B of H7 under the beam intensity of 1.4×10^8 muons/spill.

5. Discussion and conclusions

Scintillating-fibre detectors with position-sensitive photomultipliers were developed for high-rate applications and all the essential parameters to operate as a tracking detector were extensively studied.

We obtained excellent time resolutions of ~ 300 ps (r.m.s.) and of ~ 280 ps (r.m.s.) from H7 and H13 detector prototypes, respectively. In spite of a large difference in the light yield, we found no significant difference in time resolution between the two detectors. This indicates that a seven-layer structure is preferable to a 13-layer one. A small number of layers facilitates the construction of the fibre bundles with better precision in the fibre geometries. H7L showed a time resolution of ~ 540 ps (r.m.s.), which was strongly impaired by signal dispersion and attenuation in the 3-m-long light guide. This result indicates that it is very important to minimize the length of the light guide when building the final detectors. The big difference in time resolution between H7 and H7L in contrast to the small difference between H7 and H13 implies that time resolution is much more affected by the time dispersion of light signals propagating inside fibres with different angular divergences than by the time dispersion related to the number of photoelectrons.

The present study showed the excellent performance stability of the SciFi detector under high-rate conditions. The time and spatial resolutions as well as the detection efficiency were almost unchanged under different beam fluxes of 1.4×10^8 and 1×10^7 muons/spill. The stability of the pulse amplitude showed that the booster ensures stable operation of the PSPM under the high-rate conditions, providing high tracking performances.

Acknowledgements

We are grateful to the members of the CERN PS and SPS groups who arranged the best beam conditions for us during several test periods. We also recognize the endeavours of our colleagues from the COMPASS Collaboration and staff in the collaborating institutes. In particular, we deeply appreciate the many stimulating discussions of colleagues from Bonn and Erlangen universities in Germany. This work was fully supported by the Japanese Ministry of Education, Science and Culture and by the Japan Society for the Promotion of Science.

Appendix A. Magnetic shielding for the PSPM

The variation of the output pulse height of the H6568 PSPM as a function of the external magnetic field was studied in a range of magnetic shielding configurations. There are two aspects to the influence of magnetic field on the performances of the PSPM: one is the deterioration of photoelectron collection efficiency and the other is the reduction of the amplification. In the case of the present study, these two effects are not separately observable. The measurements were performed using a laboratory Helmholtz solenoid magnet which provides a field of 400 G at the maximum current of 10 A. The PSPM was oriented in different ways inside the solenoid bore. The direction of the magnetic field at different measurements (X, Y and Z) is defined with respect to the dynode structure as shown in Fig. 20. At each measurement the scan of the magnetic field was done in a cycle $0\,\text{G} \rightarrow +400\,\text{G} \rightarrow 0\,\text{G} \rightarrow$

−400 G→0 G to check the hysteresis effects. The pulse heights of the signals from the last dynode and anode channel No. 10 were measured simultaneously at each given magnetic field by using a digital oscilloscope. The light source was a red LED periodically flashing in short pulses, each producing about 50 photoelectrons over all the illuminated photocathode pixels.

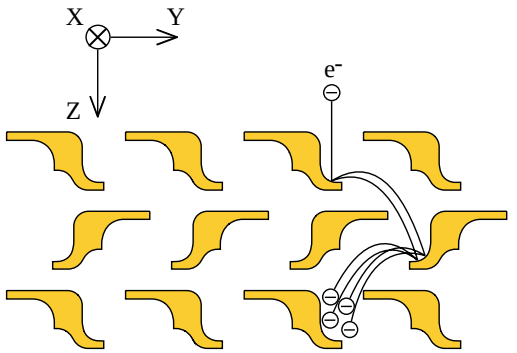

Fig. 20. Dynode structure of the H6568 and coordinate system.

The effect of magnetic field on the PSPM without any shielding was measured for the axial (Z) and transverse (X and Y) fields; the results are shown in Fig. 21. The results on the last dynode signal (triangle) and the anode signal (circle) are plotted for each field orientation. For a clear understanding of the hysteresis effects, full and open markers are used for the amplitudes obtained with the upward field scan (from negative to positive) and downward field scan (positive to negative), respectively. All the results are normalized in such a way that the pulse height at the starting point of each measurement corresponds to 100. The last dynode signal and the anode signal

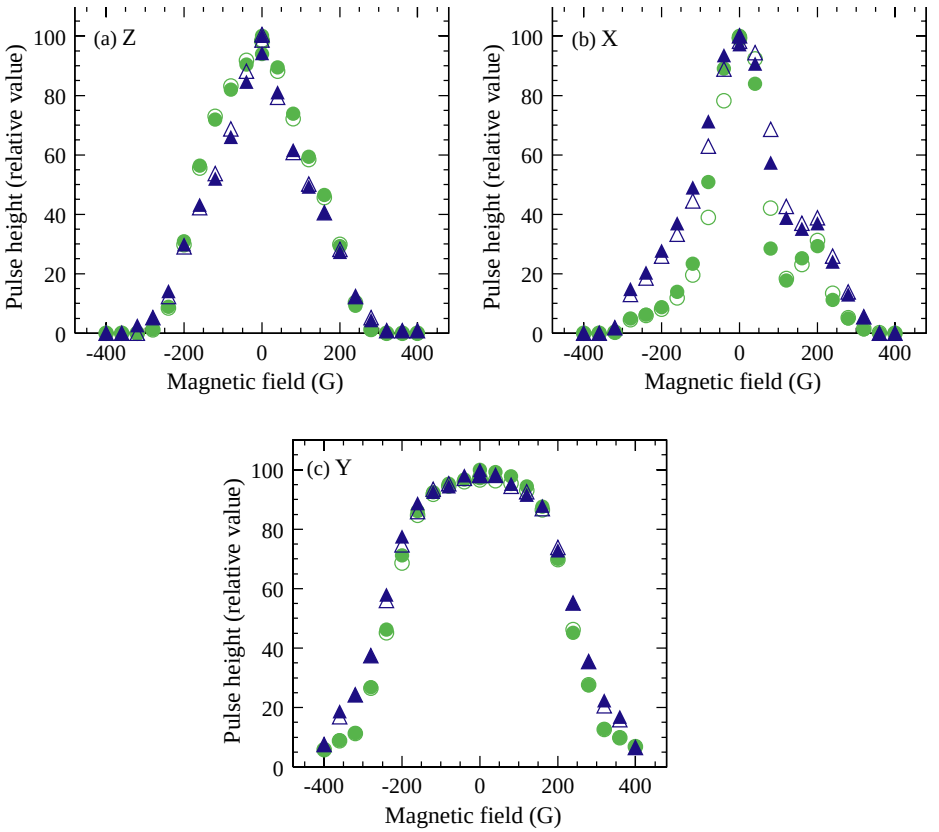

Fig. 21. Variation of the output pulse height of the H6568 in (a) Z, (b) X and (c) Y magnetic fields for the last dynode (triangle) and anode No. 10 (circle).

showed similar dependence on the external field in each orientation. It is clear that this PSPM tube shows very high immunity to a relatively small magnetic field of up to about 50 G, where the drop of the pulse height was of the order of 20% in the worst case. The immunity to the field in the Y direction is particularly high: the drop was of less than 10% without any shielding even at a field of about 120 G. The results we obtained almost agree with those given in the range of ± 100 G by the manufacturer [22]. It is worthwhile to note that their results show the influence of magnetic field on the anode signals to be dependent on the channel position within the tube.

The effects of the magnetic shielding for the PSPM were studied under similar experimental conditions. A square steel tube with dimensions $40 \times 40 \times 100$ mm^3 and 2.3 mm wall thickness was initially used as the shielding. Several measurements for different distances d between the photocathode window and the edge of the shielding tube were done under the axial magnetic field. The variation of the pulse height of the signals from the last dynode are shown in Fig. 22 for $d =$ 25 mm (circle) and $d = 45$ mm (triangle). For this geometry, the results were almost unchanged when d was more than ~ 40 mm. With such shielding the PSPM can operate without significant gain drop at

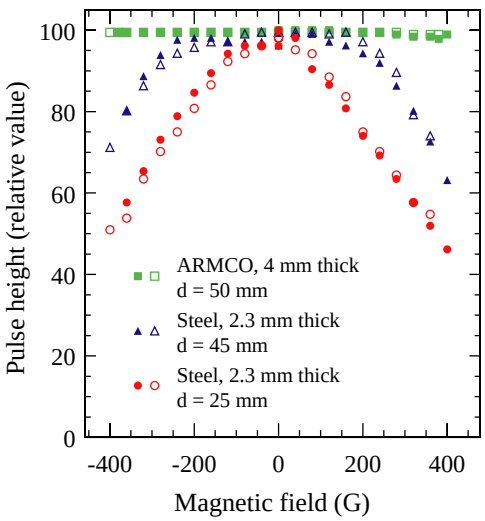

Fig. 22. Variation of the output pulse height with square iron tube shielding in an axial magnetic field.

up to 200 G of external magnetic field. It should be noted that for a transverse field (X and Y) this shielding worked perfectly: the pulse height was almost unchanged under a magnetic field of up to 400 G.

Permalloy and μ-metal are widely used for further reducing the magnetic field inside an iron tube. Additional shielding made of thin plates of these materials was also tested. The results showed practically no improvement compared to those obtained with the simple iron tube, confirming the high immunity of this PSPM to a weak magnetic field.

The 4 mm thickness of ARMCO (99.99% Fe) supplies good shielding up to 400 G, as shown by the squares in Fig. 22. The drop of the pulse height was of the order of 2% at the maximum field.

References

[1] V. Agoritsas, et al., Nucl. Instr. and Meth. A 406 (1998) 393.
[2] P. Annis, et al., Nucl. Instr. and Meth. A 412 (1998) 19.
[3] B.B. Back, et al., Nucl. Instr. and Meth. A 412 (1998) 191.
[4] M. Altmeier, et al., Nucl. Instr. and Meth. A 431 (1999) 428.
[5] J. Bähr, et al., Nucl. Instr. and Meth. A 442 (2000) 203.
[6] W. Baldini, et al., Nucl. Instr. and Meth. A 461 (2001) 219.
[7] T. Okusawa, et al., Nucl. Instr. and Meth. A 459 (2001) 440.
[8] V. Agoritsas, et al., Nucl. Instr. and Meth. A 411 (1998) 17.
[9] A. Gorin, et al., Czech. J. Phys. 49 (1999) 173.
[10] COMPASS Proposal CERN/SPSLC 96-14, SPSLC/P297, CERN, 1 March 1996.
[11] S. Horikawa, et al., Nucl. Instr. and Meth. A 431 (1999) 177.
[12] I. Daito, et al., Nucl. Instr. and Meth. A 433 (1999) 587.
[13] S. Horikawa, et al., IEEE Trans. Nucl. Sci. NS-49 (2002) 950.
[14] J. Bisplinghoff, et al., Nucl. Instr. and Meth. A 490 (2002) 101.
[15] Kuraray Technical Information, Scintillation Materials, Kuraray Co., Ltd., Nihonbashi, Chuo-ku, Tokyo 103-0027, Japan.
[16] A. Gorin, et al., Nucl. Instr. and Meth. A, to be submitted.
[17] Hamamatsu Technical Information, Multianode photomultiplier assembly H6568, H6568-10, March 1997.
[18] J.L. Rosen, Nucl. Instr. and Meth. A 408 (1998) 191.
[19] A. Gorin, et al., Nucl. Instr. and Meth. A 452 (2000) 280.
[20] A. Gorine, et al., Nucl. Instr. and Meth. A 421 (1999) 60.
[21] H. Fischer, et al., Nucl. Instr. and Meth. A 461 (2001) 507.
[22] Hamamatsu Technical Information, private communication.